Geophysical Journal International

Geophys. J. Int. (2015) **203,** 2277–2286 doi: 10.1093/gji/ggv424
GJI Seismology

Theoretical study on the amplitude ratio of the seismoelectric field to the Stoneley wave and the formation tortuosity estimation from seismoelectric logs

Wei Guan, Chenggang Yin, Jun Wang, Naigang Cui, Hengshan Hu and Zhi Wang

School of Astronautics, Harbin Institute of Technology, P.O. Box 344, *No.* 92 *West Dazhi Street, Harbin* 150001, *China. E-mail: wangjun2012@hit.edu.cn*

Accepted 2015 September 30. Received 2015 September 29; in original form 2015 January 6

SUMMARY

Seismoelectric logging has potential applications in exploring the porous formation characteristics. In this study, we theoretically address how the amplitudes of the Stoneley wave and its accompanying borehole seismoelectric field depend on the porous formation parameters such as porosity, permeability and tortuosity. We calculate the ratio of the electric field amplitude to the pressure amplitude (REP amplitude) for the low-frequency Stoneley wave of different formations and find that the REP amplitude is sensitive to porosity and tortuosity but insensitive to permeability. To confirm this conclusion, we derive the approximate expression of the REP amplitude in the wavenumber–frequency domain which shows that the REP amplitude is dependent on tortuosity but independent of permeability. This contradicts the result concluded by previous researchers from experiments that the REP amplitude is directly proportional to the permeability. The reason is probably attributed to the fact that the rock samples with different permeabilities typically have different tortuosities. Since the REP amplitude is sensitive to tortuosity, we propose a method of estimating formation tortuosity from seismoelectric logs. It is implemented by using the REP amplitude and the wavenumber of the Stoneley wave at a given frequency when the porosity and the pore fluid viscosity and salinity are known. We test the method by estimating the tortuosities from the synthetic seismoelectric waveforms in different formations. The result shows that the errors relative to the input tortuosities are lower than 5.0 per cent without considering the uncertainties of other input parameters.

Key words: Downhole methods; Guided waves; Wave propagation.

INTRODUCTION

Tortuosity of a porous formation has geophysical significance of bridging the microscopic pore-structure and some macroscopic properties like porosity, permeability and conductivity. The specific definitions and formulas of tortuosity can be found in previous works (e.g. Johnson *et al*. 1987; Revil 2013), according to fluid flow or electric conduction in a porous medium. The tortuosity can be independently measured by either acoustic or electrical method in laboratory. Using the acoustic index of refraction of superfluid ^{4}He, Johnson *et al*. (1982) experimentally measured the tortuosities of fused-glass-bead samples saturated with He II. Under the high-salinity condition of neglecting the surface conductivity, the tortuosity (α_∞) can also be determined from the porosity (ϕ) and the conductivities of the pore fluid (σ_w) and of the fluid-saturated porous medium (σ_0), according to the formulas of $F = \sigma_w/\sigma_0$ (Archie 1942) and $\alpha_\infty = F\phi$ (e.g. Brown 1980), where F is formation factor. In this study, a potential method of evaluating tortuosity from seismoelectric logs is presented, which is expected to be useful in obtaining formation tortuosity continuously in downhole and helpful for estimating permeability from seismoelectric logs (Guan *et al*. 2013a).

The seismoelectric logging is a potential technology proposed for detecting formation properties in petroleum exploration field (e.g. Zhu *et al*. 1999). It derives from the electrokinetic coupling between elastic and electromagnetic wavefields having the origin of the pore fluid flow in the electric double layer of a fluid-filled porous medium. The underground rock is typically porous and filled with electrolyte solution. There is an electric double layer with excess charges at the solid and fluid interface, which consists of a Stern layer and a diffuse layer (e.g. Revil & Glover 1997; Leroy & Revil 2004). The sorbed charges on the mineral surface are counterbalanced by the excess charges in the Stern layer and in the diffuse layer, which can be totally or partly dragged by the flow of the pore water with respect to the mineral skeleton. In the seismoelectric logging, an acoustic transmitter is used similar to that in the acoustic logging, which radiates acoustic waves traveling through the borehole liquid to the porous formation where the electrokinetic effect occurs. Because of the propagating elastic waves in the porous medium, a relative movement between the solid matrix and the pore fluid is

generated, which carries the net charges in the electric double layer and leads to an advected electric current and an electromagnetic field. As a result, not only the pressure transducers are employed to record the acoustic waves but also the electrodes are set to sense to electric potential difference in the borehole. Using the recorded electromagnetic signals and their relations with the recorded borehole acoustic signals, it is hopeful that the formation can be better characterized than using the acoustic signal alone.

To study the electrokinetic phenomena theoretically on the basis of previous works, Pride (1994) derived a set of governing equations for the coupled seismic and electromagnetic fields in fluid-saturated porous media. Although the surface conductivity of the Stern layer is neglected in his work due to no description of the conduction and polarization of the Stern layer (Revil *et al*. 2011), both theoretical and experimental works were developed for investigating the borehole seismoelectric logs by using Pride's equations. Zhu *et al*. (1999) first measured the seismoelectric signals in small-scaled model wells, in which two kinds of seismoelectric wavefields predicted by Haartsen & Pride (1997) were recorded, one is the stationary electric field accompanying the acoustic waves and the other is the independently propagating electromagnetic wave. Following that, further experimental measurements in laboratory or in field were reported by Hunt & Worthington (2000), Mikhailov *et al*. (2000), Zhu & Toksöz (2003, 2005), Singer *et al*. (2005) and so on. To solve Pride's equations in the cylindrical coordinate system, Hu *et al*. (2000) first derived the expressions of the seismoelectric wavefields in the borehole and the porous formation outside the borehole and simulated the full waveforms of the seismoelectric logging with an acoustic point source centred in the borehole. Mikhailov *et al*. (2000) experimentally recorded the Stoneley-wave induced electric field excited by vertically striking the casing with a sledge hammer at the top of a well, and theoretically derived an approximate expression of the ratio of the electric field to the pressure (REP) from Tang *et al.*'s (1991) simplified formula for the low-frequency Stoneley wave. Hu & Liu (2002) proposed a simplified approach to simulating seismoelectric logs, which calculates the borehole acoustic wave separately before solving the electric field due to the negligible influence of the induced electric field on the seismic field itself in the formation. Following that, theoretical works were focused on the full waveforms simulations in different models or by different algorithms (e.g. Pain *et al*. 2005; Hu *et al*. 2007; Guan & Hu 2008; Guan *et al*. 2013b), which lack enough analysis of the relationships between seismoelectric logs and rock physical characteristics and effective guidance to extract formation information from electrokinetic logs.

By means of the synthetic full waveforms, Hu *et al*. (2000) investigated the influence of permeability on the time-domain wave-amplitude ratio of the converted electric field to the pressure for the Stoneley wave. As a result, they saw no advantage of seismoelectric logging over conventional acoustic logging for permeability evaluation, because such REP amplitude changes so little with permeability. This agrees with the analytical expression given by Mikhailov *et al*. (2000) of the REP amplitude, which is independent of permeability. Plyshchenkov & Nikitin (2010) theoretically investigated that the ratio of the real part to imaginary part of the REP in frequency domain is sensitive to permeability and has a potential application in permeability inversion. From the component-wave analysis by calculating the pole residue of the Stoneley wave, Wang (2010) also confirmed that the REP amplitude of the low-frequency Stoneley wave is insensitive to permeability but in contrast the REP argument is sensitive to permeability. Following these works, Guan *et al*. (2013a) proposed a method of using the tangent of the REP argument of the seismoelectric logs to estimate formation permeability. However, the relation between the REP and the permeability based on Pride's equations mentioned in the above papers contradicts the conclusions that the REP amplitude is sensitive to permeability given by Singer *et al*. (2005) according to both the synthetic seismoelectric logs by using Pride's theory and the experimental measurements for rock samples with different permeabilities.

In this study, we observe the relationship between the REP amplitude and various formation parameters on the basis of Pride's theory and find that the REP amplitude is sensitive to porosity and tortuosity but insensitive to permeability. The possible reason why different REP amplitudes are measured for the rock samples with different permeabilities in Singer *et al*. (2005) is that these rock samples have different tortuosities and the REP amplitude is sensitive to tortuosity. The similar explanation was also given by Zhu & Toksöz (2015) recently, in which different REP amplitudes are measured in the two directions of permeability anisotropy for artificial rock samples. Furthermore, we present a tortuosity estimation method of using the low-frequency seismoelectric logs. According to the formula proposed in this study, the tortuosity can be estimated from the REP amplitude. This is helpful for the permeability inversion from the seismoelectric logs (Guan *et al*. 2013a), in which the permeability can be estimated from the REP phase when the tortuosity and other parameters such as the porosity are known. Besides that, the estimated tortuosity is helpful to estimate the formation permeability more accurately according to some empirical formulas, such as the Kozeny's equation (e.g. Mavko *et al*. 1998) and that given by Revil *et al*. (2014).

The paper is organized as follows. First, we review the full waveform simulation of the seismoelectric logs by using Pride's equations. The amplitude variations of the Stoneley wave, the induced electric field and the REP resulting from different porosities and permeabilities are shown and compared with those in Singer *et al*. (2005). Then we analyse the sensitivities of the REP amplitude in the frequency domain to all the input parameters by using the component-wave calculation algorithm. It is found that the low-frequency REP amplitude is sensitive to tortuosity but insensitive to permeability. And then we derive the approximate expression of the low-frequency REP amplitude, by using which we obtain the tortuosity estimation formula. After that, we present the process for the tortuosity estimation and calculate the tortuosities from the simulated full waveforms of the seismoelectric logs in different formations. Finally, we discuss the application of the method and conclude this study.

Full-waveform simulation of seismoelectric logs

This study refers to the seismoelectric logging model diagrammed in Fig. 1. For simplicity, the size of the logging tool is not considered and thus its impact on the borehole wavefields is ignored in the following simulations. A point acoustic source is assumed to be located on the axis of the fluid-filled borehole with a radius of $r_b = 0.1$ m. Two arrays of pressure transducers and electrodes are set along the borehole axis in order to respectively record the pressure and the seismoelectric signals coming back into the borehole. A cylindrical coordinate system (r, θ, z) is established for simulation, whose z axis coincides with the borehole axis and the origin is at the location of the source.

According to Pride's theory (Pride 1994), the electrokinetic coupling between elastic and electromagnetic wavefields in an isotropic,

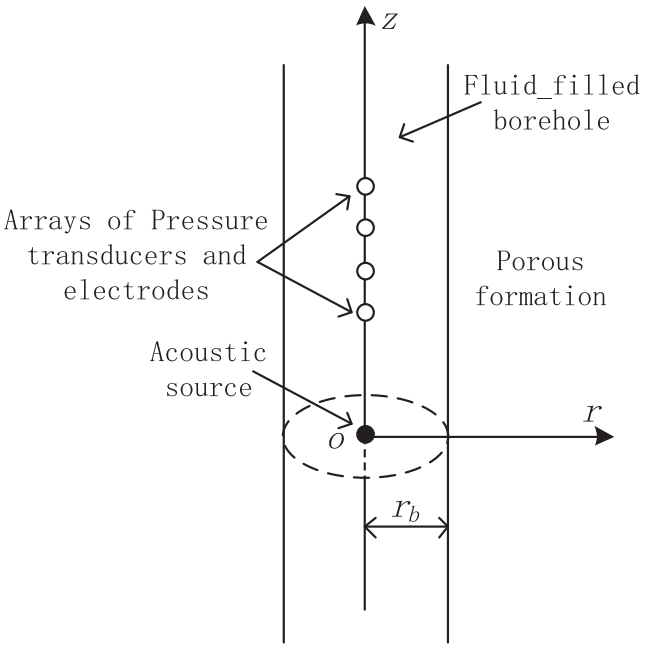

Figure 1. A schematic view of the seismoelectric logging model.

homogeneous fluid-saturated porous medium is formulized in frequency domain as follows, assuming an $e^{-i\omega t}$ time dependence:

$$\mathbf{J} = \sigma(\omega)\mathbf{E} + L(\omega)\left(-\nabla p + \omega^2 \rho_f \mathbf{u}\right) \tag{1}$$

$$-\mathrm{i}\omega\mathbf{w} = L(\omega)\mathbf{E} + \left(-\nabla p + \omega^2 \rho_f \mathbf{u}\right)\kappa(\omega)/\eta, \tag{2}$$

where i is the imaginary unit, ω is the angular frequency, t is the time, $\mathbf{E}$ and $\mathbf{J}$ are the electric field and the electric current density, respectively, $\mathbf{u}$ is the displacement of the solid phase, $\mathbf{w}$ is the relative displacement between the fluid and the solid phase, p is the pore fluid pressure, ρ_f and η are the density and the viscosity of the pore fluid, κ is the dynamic permeability defined by Johnson *et al*. (1987), and σ and L are the dynamic conductivity and the electrokinetic coupling coefficient whose expressions have been given by Pride (1994). The coupling between the elastic and electromagnetic fields is reflected in eqs (1) and (2) through the terms $L(-\nabla p + \omega^2 \rho_f \mathbf{u})$ and $L\mathbf{E}$ with the coefficient L. It can be seen that the pressure gradient term ∇p and the inertial force $\omega^2 \rho_f \mathbf{u}$ cause the electric current density $\mathbf{J}$ and the electric field $\mathbf{E}$ induces the filtration velocity $-\mathrm{i}\omega\mathbf{w}$. If L is set to be zero, the elastic and electromagnetic fields in the porous medium are decoupled, and thus Pride's electrokinetic equations break up into Biot's poroelastic wave equations (Biot 1962) and Maxwell's electromagnetic wave equations.

To solve Pride's equations under the cylindrical coordinate system as shown in Fig. 1, where the boundary conditions on the borehole wall are employed, we can obtain the simulated seismoelectric logs (e.g. Hu *et al*. 2000). Note that the wavefields at arbitrary locations in the borehole fluid and even in the porous formation can be calculated, although only those on the borehole axis are concerned in this study. In the following simulations, a monopole pressure source is employed which has a cosine wave oscillating within an envelope and an assumed intensity of peak-pressure being 1.0 Pa at 1 mm away from the source centre. The parameters of the borehole fluid and the porous formation listed in Table 1 are employed unless explicitly stated elsewhere. Regarding the parameters in Table 1, the density ρ_s and the moduli K_s, K_b and G_b are given according to the formulas fitted by Vernik (1994) from the experimental data for sandstones with different porosities. For the formation with the porosity being 0.2, the permeability is set to be 1.0 Darcy on the basis of the laboratory-measurement data for Fontainebleau sandstones given by Gomez *et al*. (2010), and the tortuosity is assumed to be 5.0 according to $\alpha_\infty = 1/\phi$ which is derived by substituting $F = \alpha_\infty/\phi$ (e.g. Brown 1980) into the Archie empirical formula $F = 1/\phi^2$ (Archie 1942). Note that the values of input parameters do not influence the following analysis of the seismoelectric logs in this study.

An example of the full waveforms of the seismoelectric logs is shown in Fig. 2. The source centre frequency is $f_0 = 6$ kHz. The waveforms in Fig. 2(a) are the pressure p (dashed dot lines) and the z-component electric field E_z (solid lines) at different receivers, which are normalized with respect to the peak values of the responses at the location of receiver-to-source distance $z = 0.5$ m. More details at $z = 3.0$ m are given in Fig. 2(b). It is seen that there are three different wave groups in the pressure waveforms, shown respectively by the dashed lines b-b, c-c and d-d in Fig. 2(a). In order of arrival time, they are the compressional wave, the shear and pseudo-Rayleigh wave and the Stoneley wave. In the electric field waveforms, there are three corresponding wave groups which are the stationary electric field accompanying the three propagating acoustic wave groups with no extent outside the acoustic pulses. Besides that, there is a wave group in the electric field waveforms which arrives earlier than the compressional wave and reaches the

Table 1 Input medium parameters for seismoelectric log simulations.

Parameter	Property	Value
ϕ	Porosity (per cent)	20
κ_0	Static Darcy permeability (mD)	1000
α_∞	Tortuosity	5.0
K_b	Frame bulk modulus (GPa)	14.39
G_b	Frame shear modulus (GPa)	13.99
K_s	Solid bulk modulus (GPa)	35.70
K_f	Pore fluid bulk modulus (GPa)	2.25
ρ_s	Solid density (kg m^{-3})	2650
ρ_f, ρ_b	Pore fluid density, borehole fluid density (kg m^{-3})	1000
C_f, C_b	Pore fluid salinity, borehole fluid salinity (mol L^{-1})	0.01
σ_f, σ_b	Pore fluid conductivity, borehole fluid conductivity (S m^{-1})	9.28×10^{-2}
ε_f, ε_b	Pore fluid permittivity, borehole fluid permittivity (F m^{-1})	7.08×10^{-10}
η	Pore fluid viscosity (Pa·s)	10^{-3}
r_b	Borehole radius (m)	0.1
v_{ba}	Acoustic velocity in borehole fluid (m s^{-1})	1500

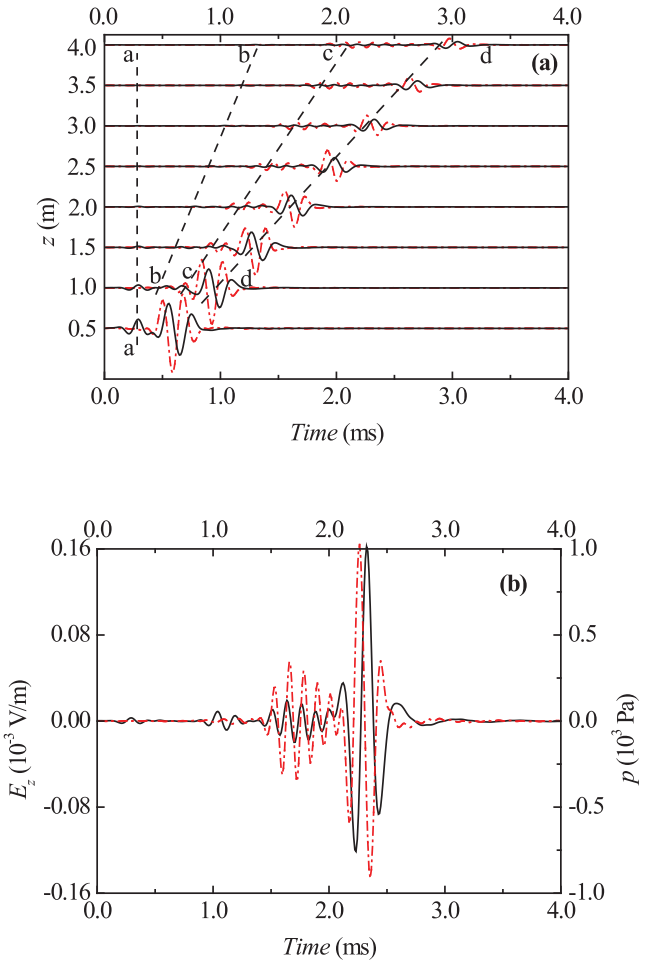

Figure 2. Full waveforms of the pressure p (dashed dot lines) and the electric field E_z (solid lines) of the seismoelectric logs with 6.0 kHz source centre frequency. (a) $z = 0.5$–4.0 m, the dash lines with a, b, c and d denote four different wave groups in the full waveforms. (b) $z = 3.0$ m.

different receivers almost at the same time [shown by the dashed line a-a in Fig. 2(a) and can be more clearly seen in Fig. 2(b)]. This wave group whose amplitude is orders of magnitude smaller than the others is an independently propagating electromagnetic wave generated by the acoustic waves when hitting on the borehole wall.

Fig. 3 shows a comparison of the amplitude variations with different porosities and permeabilities between the Stoneley wave and its induced electric field. Because of the focus on the Stoneley wave, the source with a centre frequency of 1.0 kHz is employed for the calculation in Fig. 3. At this range of frequencies, the compressional, the shear and the pseudo-Rayleigh waves are not very well excited, while the Stoneley wave dominates the full waveforms and its amplitude is significantly greater than that of the source frequency being 6.0 kHz. Figs 3(a) and (b) show the peak amplitude of the Stoneley wave group in the p and E_z waveforms, respectively. By comparing Fig. 3(a) with Fig. 3(b), it can be observed that the variation of the electric field amplitude with permeability is roughly similar to that of the pressure amplitude. Both of the two amplitudes decrease with the increasing permeability except for extremely low permeability ($\kappa_0 < 1.0$ milliDarcy) at which the electric field amplitude increases slightly. Furthermore, the amplitude-decent rates increase gradually with permeability, which means that both the electric field and the pressure amplitudes decrease more significantly for highly permeable formations. However, the electric field

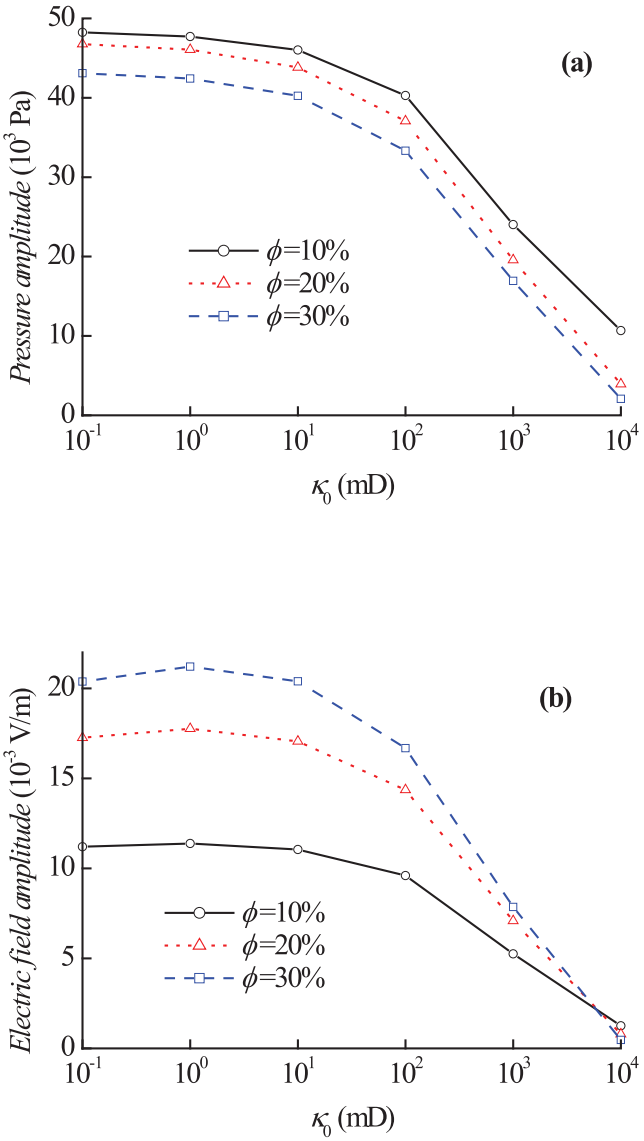

Figure 3. Peak-amplitude variations with different porosities and permeabilities of the pressure and the electric field full waveforms with 1.0 kHz source centre frequency. (a) The pressure and (b) the electric field.

and the pressure amplitudes present distinct variation tendencies for porosity. The pressure amplitudes at arbitrary permeabilities decrease with the increase of porosity. While the electric field amplitudes increase with the increasing porosity except for those at extremely high permeabilities which decrease with porosity. The reason for the variation of the electric field amplitude with porosity has been given by Guan *et al.* (2013a) in detail. It can also be found from the comparison between Figs 3(a) and (b) that the sensitivity of the electric field amplitude to the porosity is higher than that of the pressure to the porosity when permeability is less than 1.0 Darcy.

In Fig. 4, the REP amplitudes are presented by dividing the electric field amplitudes in Fig. 3(b) to the pressure amplitudes in Fig. 3(a) at the same porosities and permeabilities. It is observed that the REP amplitude changes slightly with permeability except for extremely high permeabilities ($\kappa_0 > 1.0$ Darcy) where it decreases with permeability, while it increases remarkably with the increasing porosity. This indicates that the REP amplitude calculated from Pride's equations is generally insensitive to permeability but

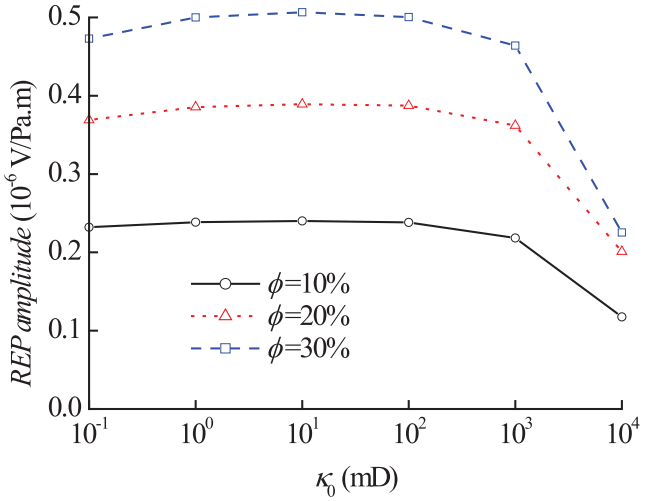

Figure 4. Variation of the REP amplitude with different porosities and permeabilities obtained by dividing the pressure amplitude by the electric field amplitude at the same porosity and permeability in Fig. 3.

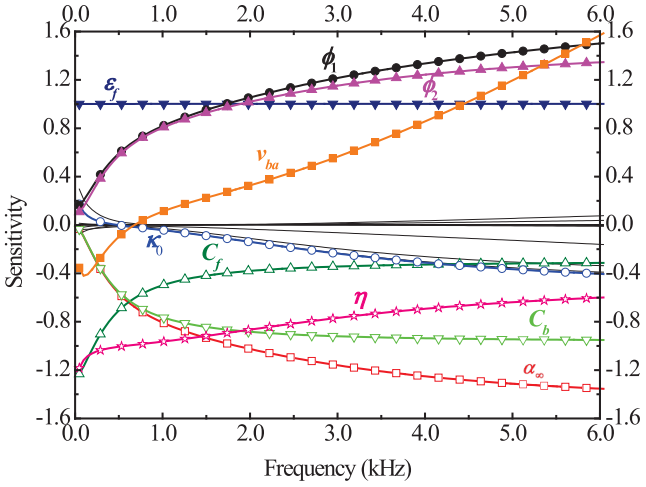

Figure 5. Sensitivities of the REP amplitude to all the input parameters listed in Table 1.

sensitive to porosity, which agrees with the expression derived by Mikhailov *et al*. (2000) where the REP amplitude is directly proportional to porosity but independent of permeability. Furthermore, the sensitivity of the REP amplitude to porosity for commonly permeable formations ($\kappa_0 < 1.0$ Darcy) is significantly higher than that of the Stoneley wave. Nevertheless, the variation tendency in Fig. 4 contradicts that given by Singer *et al*. (2005). In their works, the REP amplitudes both calculated from Pride's theory and measured in the modelled sandstone boreholes were declared being directly proportional to permeability, and thus a conclusion was drawn that the REP amplitude which is sensitive to permeability has a potential application in permeability inversion. In order to make this contradiction clear, we compare the results shown in Fig. 3 with those calculated by Singer *et al*. (2005) carefully. It is found that the variations of the electric field amplitude are quite similar between each other, while the pressure amplitude variations have a distinct difference resulting in the contrasting variations of the two REP amplitudes with permeability. Although both of the pressure amplitudes in Fig. 3(a) and in Singer *et al*. (2005) decrease with the increasing permeability, the former decrease is more significant for high-permeability formations, while the latter one is more significant for low-permeability formations. Considering that such a difference may be caused by the use of different parameters for simulation, we have recalculated the pressure, the electric field and the REP amplitudes by employing the same input parameters as those in Singer *et al*. (2005). As a result, all the variations are consistent with those in Figs 3 and 4. Actually, it is reasonable that the pressure-amplitude variation is more significant for high-permeability formations, which means that the Stoneley wave amplitude is more sensitive for high permeabilities. This agrees with the theoretical and field measured results given by Wu *et al*. (1995), where the sensitivity of the Stoneley-wave attenuation to permeability is relatively higher for high-permeability formations. Thus it is correct that the REP amplitude based on Pride's theory is not directly related to permeability.

Sensitivity analysis of the REP amplitude

In order to give a reasonable explanation of the contradiction with the measurements of Singer *et al*. (2005), the sensitivities of the REP amplitude to all the input medium parameters listed in Table 1 are calculated in this section. The sensitivity, which is defined by Cheng *et al*. (1982) and named as partition coefficient, is expressed as

$$\text{Sensitivity} = \frac{\partial M_{\text{REP}}(\omega)}{\partial x} \frac{x}{M_{\text{REP}}(\omega)} \tag{3}$$

where x denotes an input parameter such as porosity, permeability, salinity and so on, and $M_{\text{REP}}(\omega)$ is the frequency-dependent modulus of the REP amplitude. For completeness it is noted that the following sensitivity calculations are implemented by using the component-wave analysis algorithm to calculate the residues of the borehole pressure and electric field functions at the Stoneley wave pole (Wang 2010).

Because a small increment is independently set for each parameter, a positive sensitivity in Fig. 5 indicates that the REP amplitude is directly proportional to this parameter. It is seen that the REP amplitude is relatively sensitive to porosity (ϕ), tortuosity (α_∞), pore fluid viscosity (η), salinity (C_f) and permittivity (ε_f), borehole fluid salinity (C_b) and acoustic velocity in the borehole fluid (v_{ba}). Different coloured lines employed and the corresponding names labelled in Fig. 5 are to clearly show the variations of these highly sensitive parameters with frequency. Other parameters to which the sensitivity is not relatively significant are not labelled.

Compared with the highly sensitive parameters mentioned above, the sensitivity of the REP amplitude to permeability is relatively small. There is a frequency between 0.5 and 1.0 kHz in Fig. 5 where the sensitivity is zero, that is, the REP amplitude is independent on permeability at this frequency. This agrees with the results obtained from the full-waveform simulation at 1.0 kHz in Fig. 4, in which the REP amplitude is insensitive to permeability. Below the zero-sensitivity frequency, the REP amplitude is in direct proportion to permeability and the sensitivity decreases with the increasing frequency. Above the zero-sensitivity frequency, however, the REP amplitude is in inverse proportion to permeability and the sensitivity increases with the increasing frequency but it is still not significant when frequency comes up to 6.0 kHz. It is not necessary to analyse the sensitivity to permeability at higher frequencies because of the small Stoneley wave amplitude.

The REP amplitude is directly proportional to porosity, which agrees with the results in Fig. 4. Furthermore, the sensitivity of the REP amplitude to porosity increases with frequency. Note that there are two lines with respect to the sensitivity to porosity, which are labelled by ϕ_1 and ϕ_2 respectively in Fig. 5. The former is the

case of porosity changing independently on other parameters and the latter is of the moduli K_s, K_b and G_b changing simultaneously with porosity according to the relations given by Vernik (1994). The discrepancy between the two lines increases with frequency but is not significant. It indicates that the influence of the modulus K_s, K_b or G_b on the REP amplitude is small, especially when frequency is lower than 1.0 kHz. Among the three moduli, the sensitivities to G_b and K_b are respectively the first and second highest and the sensitivity to K_s is close to zero. The reason of $\phi_1 > \phi_2$ is the inverse proportion of the REP amplitude to G_b.

It is observed from Fig. 5 that the sensitivity of the REP amplitude to tortuosity is significant and increases with the increasing frequency. The negative values in the whole frequency range indicate that the REP amplitude is inversely proportional to tortuosity. Tortuosity, which is defined as a parameter relating to the microscopic pore-structure, has a significant effect on the relative flow of pore fluid. Qualitatively, a high-tortuosity porous formation generally has a low permeability. Thus we think that the immediate cause of the experimental results in Singer *et al*. (2005) is the sensitivity of the REP amplitude to tortuosity. Singer *et al*. (2005) did not provide the tortuosity data of the rock samples. Nevertheless low tortuosities are generally associated with the high permeabilities and vice versa, such as the 23 Fontainebleau sandstones given in Gomez *et al*. (2010). We thus predict that the rock samples with high permeabilities used in Singer *et al*. (2005) may have low tortuosities, which results in larger REP amplitudes and the direct proportion of the REP amplitude to permeability.

Similarly, the cases of other highly sensitive parameters can also be analysed from Fig. 5. The REP amplitude is in inverse proportion to the viscosity and salinity of the pore fluid and to the salinity of the borehole fluid, while it is in direct proportion to the permittivity of the pore fluid. With the increasing frequency, the sensitivities to the pore-fluid viscosity and salinity decrease, while that to the borehole-fluid salinity increases. The sensitivity to the pore-fluid permittivity is independent of frequency. Similar to that of the permeability, there is also a zero-sensitivity frequency of the sensitivity to acoustic velocity in borehole fluid. With the increasing frequency, the sensitivity to the acoustic velocity in borehole fluid decreases first and then increases when the frequency exceeds the zero-sensitivity frequency. Furthermore, the zero-sensitivity frequency of the acoustic velocity in borehole fluid is the same as that of the permeability. The REP amplitude is first in inverse proportion and then in direct proportion to the acoustic velocity in borehole fluid, which is opposite to the case of the permeability.

Approximate expression of the REP amplitude

For the purpose of investigating the relationship of the low-frequency REP amplitude with the highly sensitive parameters quantitatively, an approximate expression of the REP amplitude is presented in this section. Based on Pride's equations, the approximate expression of the REP in the frequency domain has been derived as follows (Plyshchenkov & Nikitin 2010; Guan *et al*. 2013a).

$$\mathrm{REP}(\omega) = \mathrm{i}\frac{\phi\varepsilon_f\varsigma}{\eta\alpha_\infty}\left(1 + \frac{m}{8}\frac{\mathrm{i}\omega}{\omega_c}\right)R_I, \tag{4}$$

where ς is the electric potential at the shear plane, which separates the Stern layer and the diffuse layer of the electric double layer, $m = \phi\Lambda^2/\alpha_\infty\kappa_0$ is a dimensionless parameter having little change for the majority of sedimentary rocks (Johnson *et al*. 1987) and is assumed to be 8.0 in this study, where Λ is a measure of the sizes of dynamically connected pores, $\omega_c = \phi\eta/\alpha_\infty\rho_f\kappa_0$ is a critical angular frequency separating the low-frequency viscous flow ($\omega \ll \omega_c$) from the high-frequency inertial flow ($\omega \gg \omega_c$), and the term R_I is expressed as (Guan *et al*. 2013a)

$$R_I = \frac{k_{st}\eta_{be}I_0(\eta_{be}r_0)}{I_0(\eta_{ba}r_0)\left(\mathrm{i}\omega\bar{\varepsilon}_b\cdot\eta_{em}^2 r_b\cdot Y_{em}\cdot I_1(\eta_{be}r_b) + \eta_{be}\cdot\mathrm{i}\omega\bar{\varepsilon}\cdot I_0(\eta_{be}r_b)\right)}, \tag{5}$$

where r_0 is the radial offset from the receivers to the borehole axis; k_{st} is the wavenumber of the Stoneley wave; $\eta_{ba} = (k^2 - k_{ba}^2)^{1/2}$, $\eta_{be} = (k^2 - k_{be}^2)^{1/2}$ and $\eta_{em} = (k^2 - k_{em}^2)^{1/2}$ are the radial wavenumbers in which k is the axial wavenumber, k_{be} and k_{ba} are the wavenumbers of the electromagnetic and the acoustic waves in the borehole fluid and k_{em} is the wavenumber of the electromagnetic wave in the porous formation; $\bar{\varepsilon}_b = \varepsilon_b + i\sigma_b/\omega$ and $\bar{\varepsilon} = \varepsilon + i\sigma(\omega)/\omega$ are the effective permittivities of the borehole fluid and the porous formation, respectively, in which ε_b and σ_b are respectively the permittivity and conductivity of the borehole fluid and ε is the permittivity of the porous formation. The term Y_{em} is expressed as $Y_{em} = K_0(\eta_{em}r_b)/\eta_{em}r_bK_1(\eta_{em}r_b)$, I_j and K_j ($j = 0, 1$) are modified Bessel functions of order j. The detailed derivation of eq. (5) can be found in Guan *et al*. (2013a). Note that the meanings of other parameters in eqs (4) and (5) are the same as those listed in Table 1 or appeared in the above text.

To calculate the term R_I in eq. (4) by employing the parameters in Table 1, we find that the real and imaginary parts of R_I are always positive and moreover the real part is much larger than the imaginary part if the frequency is more than 0.5 kHz. Further calculations show that such condition is always satisfied whatever the formations. Hence the term R_I is regarded as a real function approximately and then the real and imaginary parts of the REP are respectively written as

$$\mathrm{Re}\,(\mathrm{REP}) = -\frac{\phi\varepsilon_f\varsigma}{\eta\alpha_\infty}\left(\frac{m}{8}\frac{\omega}{\omega_c}\right)R_I, \tag{6}$$

$$\mathrm{Im}\,(\mathrm{REP}) = \frac{\phi\varepsilon_f\varsigma}{\eta\alpha_\infty}R_I. \tag{7}$$

Thus, according to eqs (6) and (7) the REP amplitude is expressed as

$$|\mathrm{REP}(\omega)| = \frac{\phi\varepsilon_f|\varsigma|}{\eta\alpha_\infty}R_I\sqrt{1 + \left(\frac{m}{8}\frac{\omega}{\omega_c}\right)^2}. \tag{8}$$

A sign of absolute value added to ς in eq. (8) is because the zeta potential can be negative or positive and moreover it is negative for the calculations in this paper. If the frequency is lower than several kilohertz, the low-frequency limit condition of $\omega \ll \omega_c$ is commonly satisfied for real rocks. Thus eq. (8) of the REP amplitude approximates to

$$|\mathrm{REP}(\omega)| = \frac{\phi\varepsilon_f|\varsigma|}{\eta\alpha_\infty}R_I. \tag{9}$$

Then the following three types of approximations are substituted into eq. (5) in order to simplify the term R_I reasonably. The first is $|\eta_{be}| \approx |k_{st}|$ and $|\eta_{em}| \approx |k_{st}|$. They are obtained at the Stoneley wave pole $k = k_{st}$ by considering that the electromagnetic wavenumbers in the borehole fluid and the porous formation are much smaller than that of the Stoneley wave, that is, $k_{be}^2 \ll k_{st}^2$ and $k_{em}^2 \ll k_{st}^2$. The second is $\mathrm{i}\omega\bar{\varepsilon}_b \approx -\sigma_b$ and $\mathrm{i}\omega\bar{\varepsilon} \approx -\sigma$. The pore

fluid and the porous formation are electric conductors at frequencies of several kilohertz, and thus the conduction currents are much larger than the displacement currents, that is, $\sigma_b \gg \omega\varepsilon_b$ and $\sigma \gg \omega\varepsilon$. The third is $I_0(\eta_{be}r_0) \approx 1.0$, $I_0(\eta_{be}r_b) \approx 1.0$ and $I_0(\eta_{ba}r_0) \approx 1.0$. The wavelengths of the electromagnetic and the acoustic waves in the borehole are much larger than the borehole radius, and thus their radial wavenumbers satisfy $|\eta_{be}|r_0 \ll 1.0$, $|\eta_{be}|r_b \ll 1.0$ and $|\eta_{ba}|r_0 \ll 1.0$. As a result, the REP amplitude approximates to

$$|\mathrm{REP}(\omega)| = \frac{\phi\varepsilon_f\,|\varsigma|\,k_{st}}{\eta\alpha_\infty}\left[\sigma(\omega) + \sigma_b\frac{I_1(r_bk_{st})K_0(r_bk_{st})}{I_0(r_bk_{st})K_1(r_bk_{st})}\right]^{-1}. \quad (10)$$

Note that eq. (10) of the REP amplitude has a similar form as that given by Mikhailov *et al*. (2000) in which the derivation was carried out by using the quasi-static electromagnetic condition and Tang *et al.*'s (1991) approximate formula of the low-frequency Stoneley wave.

The sensitivities calculated in Fig. 5 can be confirmed from eq. (10). It is seen from eq. (10) that the REP amplitude is directly proportional to porosity and pore-fluid permittivity but is in inversely proportional to tortuosity and pore-fluid viscosity, which agrees with the sensitivities given in Fig. 5. Note that the dependence of the REP amplitude on porosity and tortuosity or on the formation factor is not only as that explicitly shown in eq. (10) but also implicitly given by the relation of the formation factor with the formation conductivity in our calculations. According to $F = \sigma_f/\sigma_0$ and $F\phi = \alpha_\infty$, we substitutes $\sigma_0 = \sigma_f\phi/\alpha_\infty$ of the formation conductivity at low frequency limit into eq. (10) and thus we have

$$|\mathrm{REP}(\omega)| = \frac{\phi\,|\varsigma|\,\varepsilon_f k_{st}}{\eta}\frac{\left[\sigma_f\phi + \sigma_b\alpha_\infty\dfrac{I_1(r_bk_{st})K_0(r_bk_{st})}{I_0(r_bk_{st})K_1(r_bk_{st})}\right]}{1}. \quad (11)$$

Note that the quadrature conductivity and the low-frequency induced polarization (e.g. Revil *et al*. 2014) are ignored.

It is seen from eq. (11) that the monotonic properties of the REP amplitude with respect to porosity and tortuosity are not changed by the relation of the conductivity with the porosity and the tortuosity. The REP amplitude is in direct proportion to the zeta potential that depends on the parameters such as the pore fluid salinity and pH value. There exists no direct measurement of the zeta potential for rocks. The zeta potential can be derived from the measured streaming-potential coefficient (C_s) by using the well-known Helmholtz–Smoluchowski equation $C_s = \varepsilon_f\varsigma/\eta\sigma_f$ for capillary tubes although it has still never been validated for rocks (e.g. Glover *et al*. 2012). In this study, the zeta potential is calculated from the pore fluid salinity by using the experimental fitting formula of $\varsigma = 0.008 + 0.026\log_{10}(C_f)$ given by Pride & Morgan (1991). Note that such kinds of fitting formula for calculating the zeta potential can also be theoretically derived from the model of the electric double layer (Revil *et al*. 1999). Thus the REP amplitude is dependent on the pore fluid salinity, which agrees with the fact that the REP amplitude is sensitive to the pore fluid salinity shown in Fig. 5. The pore fluid salinity affects not only the zeta potential but also the pore fluid conductivity, thus it affects the conductivity of the porous formation which is related to the REP amplitude as shown in eq. (10). Similarly, the REP amplitude is dependent on the conductivity of the borehole fluid and thus it is sensitive to the salinity of the borehole fluid as shown in Fig. 5. When the salinities of the pore fluid and the borehole fluid are equal with each other as that in the calculations of Fig. 5, the conductivity of the pore fluid which is equal to that of the borehole fluid can be moved outside of the bracket in eq. (11) and thus the REP amplitude is in direct proportion to the streaming-potential coefficient C_s. According to the previous experimental results compiled by Glover *et al*. (2012), C_s is inversely proportional to the pore fluid salinity, except for low-salinity pore fluid where the effects of micro pore-structure, surface conductivity, pH values, etc. are significant. Thus, the REP amplitude is in inverse proportion to the pore fluid salinity which is the same as that shown in Fig. 5. The REP amplitude is also dependent on the wavenumber of the Stoneley wave which relates to the acoustic velocity in borehole fluid, thus it is sensitive to the acoustic velocity in borehole fluid as that shown in Fig. 5. In a word, the relationships between the low-frequency REP amplitude and the parameters in eq. (10) agree with the sensitivities shown in Fig. 5 and the relevant analysis mentioned above.

Tortuosity estimation

From eq. (11) of the approximate expression of the REP amplitude at low frequencies, a formula for estimating the tortuosity is derived in this section, by which the tortuosities are then estimated from the simulated seismoelectric logs.

In order to facilitate the following derivation, the term $I_1(r_bk_{st})K_0(r_bk_{st})/I_0(r_bk_{st})K_1(r_bk_{st})$ in the right-hand side of eq. (11) is instead by a variable $A(k_{st}, r_b)$, which can be determined from the Stoneley wavenumber k_{st} and the borehole radius r_b. Then an explicit expression of tortuosity is obtained as

$$\alpha_\infty = \frac{\frac{\phi|\varsigma|\varepsilon_f k_{st}}{\eta|\mathrm{REP}(\omega)|} - \sigma_f\phi}{\sigma_b A\,(k_{st}, r_b)}. \quad (12)$$

Based on eq. (12) and the above analysis of the REP amplitude, we propose a tortuosity estimation method of using the velocity of Stoneley wave and the REP amplitude of the low-frequency seismoelectric logs. Note that the porosity, the borehole fluid salinity and the pore fluid properties (viscosity and salinity) should be known before estimating the tortuosity. These formation properties can be measured independently from different kinds of diagraphy tools in oil exploration. For example, acoustic logging and self-potential logging can be respectively used to obtain the varying curves of porosity and fluid salinity with depth. Specifically, the borehole fluid salinity is used to calculate the conductivity of the borehole fluid. The pore fluid salinity is used to calculate both the permittivity and the conductivity of the pore fluid and to estimate the zeta potential of the electric double layer. The details of the method are elaborated as follows. (1) It is required to provide the dispersion curve of the Stoneley wave velocity and the REP amplitude with frequency. The wavenumber of the Stoneley wave and the REP amplitude in eq. (12) vary with frequency obviously, thus their values at a given frequency should be used for tortuosity estimation. We have tested to estimate tortuosities from the REP amplitude obtained directly from the time-domain waveforms of the pressure and electric field as that in Fig. 4. Consequently, the results are not accurate due to the components of different frequencies consisting in the full waveforms. To obtain the frequency-dependent REP amplitude, the pressure and electric signals received at the same location in the borehole should be Fourier-transformed from the time domain to the frequency domain. (2) It is required to employ an acoustic transmitter with a centre frequency between 1.0 kHz and 4.0 kHz. The first reason is that the Stoneley wave is well excited and dominates the full waveforms at this frequency range. Thus it is not required to extract the Stoneley wave group and the full waveforms can be directly used to obtain the dispersion curve of the REP

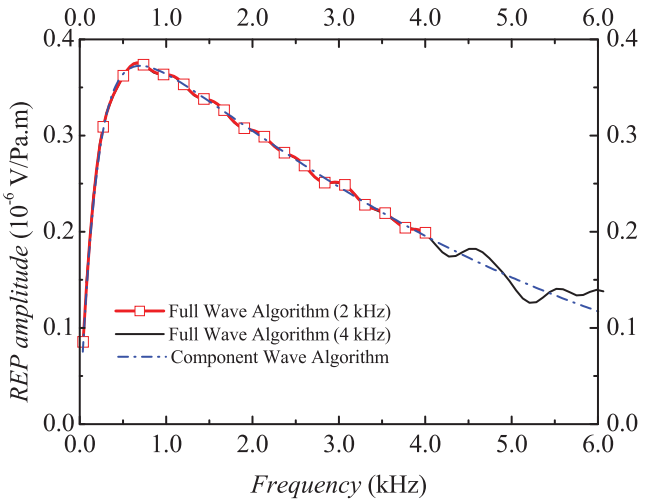

Figure 6. Comparison between the dispersion curves of the REP amplitude calculated from the component wave algorithm (Wang 2010) and Fourier-transformed from the full waveforms of different source frequencies.

amplitude. In Fig. 6, we compare the curve obtained from the component wave algorithm (Wang 2010) with those Fourier-transformed from the simulated full waveforms of different source frequencies. At the low frequency region in Fig. 6 (about lower than 500 Hz), the curves obtained by the two methods completely coincide with each other and there is no visible distinction between them. At intermediate frequencies (between 0.5 kHz and 4.0 kHz in Fig. 6) the curves are essentially coincident and the distinction is not too big, but at the high frequency region (higher than 4.0 kHz) the distinction is obvious. The reason is that the high-frequency component of the Stoneley wave is relatively small and the effect of other wave groups in the full waveform on the dispersion curves of the Stoneley wave increases at high frequencies. Note that the curve obtained from the full waveform of the 2.0 kHz source is cut off at 4.0 kHz, because the maximum frequency in our full-waveform calculation is set to be two times the centre frequency. Besides that, using a source with low frequencies which exciting a larger-amplitude Stoneley wave can induce stronger electric signals and improve the signal to noise ratio. (3) The values of the REP amplitude and the wavenumber of the Stoneley wave at frequencies between 0.5 and 1.0 kHz should be used for estimation. For one thing, several approximate conditions used for deriving the expression of the REP amplitude mentioned above, such as considering the term R_I as a real function, are satisfied when the frequency is about higher than 0.5 kHz. We have tested that the estimated tortuosity from the REP amplitude and the wavenumber of the Stoneley wave at 50 Hz differs significantly with the real values (the input tortuosity). For another, some approximate conditions are better satisfied at lower frequencies which are about higher than 0.5 kHz. We have tested that the error of the estimated tortuosity increases with the corresponding frequency of the REP amplitude and the wavenumber of the Stoneley wave used.

As listed in Table 2 the tortuosities of different porous formations are estimated from the simulated seismoelectric logs. The source whose centre frequency is 1.0 kHz is employed for simulations. The values of the REP amplitude and the wavenumber of the Stoneley wave at the frequency of 0.5 kHz are used for estimation. The estimated tortuosities and the errors relative to the input values for simulations are given in Table 2. According to its definition, the tortuosity for a porous formation should be greater than 1.0 that is for an ideal capillary. No matter the values of the porosity and permeability, the relative errors of the tortuosity being 1.0 are distinctly larger than that of the tortuosity being 3.0 or 5.0. Commonly, the sandstone with a high permeability is associated with low tortuosity and vice versa. For the formation with a relatively high permeability (1.0 Darcy), the error of the tortuosity being 3.0 or 5.0 is the lowest. For the formation with a relatively low permeability (0.01 Darcy), however, the error of relatively high tortuosity (11.0) is the lowest. When permeability is 1.0 Darcy for example, the estimated tortuosities and the relative errors are compared among porosities being 10, 20 and 30 per cent in Table 2. Except for the ideal case of tortuosity being 1.0, the relative errors decrease with the increasing porosity and that of porosity being 30 per cent are the lowest no matter the values of tortuosity because high porosity is often associated with high permeability. In general, without considering the uncertainties of other input parameters, the relative errors are lower than 5.0 per cent except for several unrealistic cases of high permeabilities with high tortuosities(the permeability, porosity and tortuosity are 1.0 Darcy, 10 per cent and 11.0 respectively) or low permeabilities with low tortuosities (the permeabilities are 0.1 Darcy and 0.01 Darcy and the tortuosity is 1.0).

DISCUSSION

It is seen from eq. (12) that an explicit expression for the formation factor can be obtained if both sides of eq. (12) are divided by porosity. In this case, the tortuosity estimation method proposed in this study can also be used to estimate the formation factor without using the porosity and then to calculate the formation conductivity if the pore fluid salinity is not very low and the effect of the surface conductivity can be ignored.

Table 2. Comparison of the estimated tortuosities of different formations with those used for simulations.

Permeability (Darcy)	1.0						0.1		0.01	
Porosity	10%		20%		30%		20%		20%	
Tortuosities used for simulations	Estimated values	Relative errors (%)	Estimated values	Relative errors (%)	Estimated values	Relative errors (%)	Estimated values	Relative errors (%)	Estimated values	Relative errors (%)
1.0	1.033	3.30	1.043	4.30	1.020	2.00	1.076	7.60	1.174	17.40
3.0	3.069	2.30	3.057	1.90	3.017	0.57	3.069	2.30	3.149	4.97
5.0	5.136	2.72	5.085	1.70	5.031	0.62	5.063	1.26	5.146	2.92
7.0	7.253	3.61	7.123	1.76	7.056	0.80	7.046	0.66	7.138	1.97
9.0	9.441	4.90	9.170	1.89	9.091	1.01	9.013	0.14	9.118	1.31
11.0	11.718	6.53	11.230	2.09	11.137	1.25	10.964	−0.33	11.084	0.76

During the derivation of eq. (12) without considering the surface conductance, the equation $\sigma_0 = \sigma_f\phi/\alpha_\infty$ based on $F\phi = \alpha_\infty$ and $F = \sigma_f/\sigma_0$ is used to substitute the formation conductivity in eq. (10). The formation factor according to $F\phi = \alpha_\infty$ is only dependent on the solid matrix but independent of the pore fluid properties. Because the clay existing in the pores affects the connectivity of pores and causes the surface conductance nearby the interface between solid matrix and pore fluid, the experimental measured σ_f/σ_0 varies with the pore fluid salinity which results in a departure of $\sigma_f\phi/\alpha_\infty$ from the formation conductivity. This departure decreases with the increasing porosity and pore fluid salinity. Nevertheless, a tortuosity estimation formula similar to eq. (12) can still be derived without using the equation $\sigma_0 = \sigma_f\phi/\alpha_\infty$. In this case of tortuosity estimation, the formation conductivity must be measured by electric logging or other methods.

The zeta potential of the electric double layer is difficult to be measured directly but it is necessary when estimating tortuosity according to eq. (12). The zeta potential formula (Pride & Morgan 1991) fitted from the streaming-potential coefficient measurement is employed in this study, which is dependent only on the pore fluid salinity. However, the pH value of the pore fluid has great influence on the zeta potential especially for the formation with low pore fluid salinity (Revil *et al*. 1999). Thus it is necessary in the future work to using the experimental fitting formula of the zeta potential dependent on both the pore fluid salinity and the pH value, such as that has been given by Revil *et al*. (1999). Nevertheless, substituting the Helmholtz-Smoluchowski equation $C_s = \varepsilon_f\varsigma/\eta\sigma_f$ into eq. (12) yields

$$\alpha_\infty = \frac{\sigma_f\left(\frac{\phi|C_s|k_{st}}{|\mathrm{REP}(\omega)|} - \phi\right)}{\sigma_b A}. \tag{13}$$

Based on eq. (13), the tortuosity can be estimated by using the measured streaming-potential coefficient C_s instead of using the zeta potential and the pore fluid viscosity. All the same, the porosity should still be known and the salinities of the borehole and the pore fluid are needed to calculate the conductivities σ_b and σ_f, respectively.

One of the important benefits of obtaining the tortuosity is to estimate permeability. According to Guan *et al*. (2013a), the tortuosity should be used for the permeability estimation from the seismoelectric logs. Moreover, although high permeability is commonly associated with high porosity, it is unreasonable to use the porosity only to estimate permeability due to the difference of microscopic pore structures. Besides that, the permeability anisotropy which is caused by the variety of pore structure in different directions cannot be expressed by a scalar function of porosity but is possible to be described by the tortuosity anisotropy. In fact, the permeability has been expressed by using the tortuosity, porosity and other parameters in pioneering studies, such as the modified Kozeny's equation (Mavko *et al*. 1998) shown as follows,

$$\kappa_0 = \frac{1}{72}\frac{(\phi-\phi_c)^3}{[1-(\phi-\phi_c)]^2{\alpha_\infty}^2}d^2, \tag{14}$$

where d is the grain diameter, ϕ_c is the percolation porosity which corresponds to that below which the remaining porosity is disconnected and does not contribute to flow. Although it has been validated that Kozeny's equation (Kozeny 1927) or its modified forms such as eq. (14) can be used to estimate the permeability in North Sea Chalks, Fontainebleau sandstones and so on (e.g. Olsen *et al*. 2008; Gomez *et al*. 2010), the accuracy is not enough even for Fontainebleau sandstones with permeabilities being less than 1.0 Darcy (Revil & Cathles 1999). In Gomez *et al*. (2010), permeabilities of 23 Fontainebleau sandstone samples were calculated from eq. (14) by using the measured porosities only but supposing $\alpha_\infty = 2.5$, $d = 250$ μm and $\phi_c = 2$ per cent. Most of the calculated permeabilities are very close to the measured nitrogen permeabilities, and the maximum difference is lower than one order of magnitude. If using the measured or estimated tortuosities instead of the supposed ones, the differences may decrease further. By using the tortuosities obtained from the measured formation factors, we have calculated that the permeabilities are 0.8 and 20 milliDarcy respectively for the samples numbered F410 and F570 in Gomez *et al*. (2010). They are more close to the measured values of 1.0 and 32 milliDarcy compared with 9.6 and 84 milliDarcy by using the supposed tortuosity. Note that not all the permeabilities by using the estimated tortuosities are more close to the measured values possibly because of the inaccuracy of the measured formation factors in Gomez *et al*. (2010).

CONCLUSIONS

In this paper, we have studied the dependence of the REP amplitude of seismoelectric logs on porous formation parameters such as porosity, permeability and tortuosity, and have proposed a tortuosity estimation method by the seismoelectric logs.

By analysing the synthetic full waveforms of the low-frequency seismoelectric logs in different formations, we have found that the REP amplitude is sensitive to porosity but insensitive to permeability. Such relations between the REP amplitude and porosity as well as permeability have been confirmed by calculating the sensitivities of the REP amplitude to all the input parameters according to the sensitivity function defined by Cheng *et al*. (1982). Besides porosity, the REP amplitude is also sensitive to tortuosity, pore fluid viscosity, salinity and permittivity, borehole fluid salinity and acoustic velocity in borehole fluid. Thus, we predicted that the contradiction of Pride's theory with the direct proportion between the REP amplitude and permeability experimentally measured by Singer *et al*. (2005) is due to the fact that the formation samples with different permeabilities have different tortuosities.

We have derived the approximate expression of the REP amplitude, which is similar to that given by Mikhailov *et al*. (2000) by using the quasi-static electromagnetic condition and Tang *et al*.'s (1991) approximate formula of the low-frequency Stoneley wave. The relations between the REP amplitude and the parameters in the expression agree with that obtained from sensitivity calculations. Based on the explicit form with respect to tortuosity, which is obtained by rewriting the expression of the REP amplitude, we have proposed the tortuosity estimation method by the low-frequency seismoelectric logs. According to this method, the tortuosity can be estimated from the REP amplitude and the wavenumber of Stoneley wave at a given frequency when the formation porosity and the pore fluid viscosity and salinity are known. We have calculated the tortuosities of different formations exactly from the simulated seismoelectric log. The obtained tortuosity is useful for the formation permeability estimation from the seismoelectric logs (Guan *et al*. 2013a) or some empirical equations such as the modified Kozeny's equation (Mavko *et al*. 1998) for sandstones.

ACKNOWLEDGEMENTS

We thank Prof André Revil, Dr Yongxin Gao and an anonymous reviewer for their revision suggestions for this paper. This work

is supported by National Natural Science Foundations of China (41574112, 41204092, 11372091 and 41174110), Natural Science Foundation of Heilongjiang Province of China (D2015001) and Postdoctoral Science Special Foundation of China (2012T50336).

REFERENCES

Archie, G.E., 1942. The electrical resistivity log as an aid in determining some reservoir characteristics, *Trans. Am. Inst. Mech. Eng.,* **146,** 54–62.

Biot, M.A., 1962. Mechanics of deformation and acoustic propagation in porous media, *J. Appl. Phys.,* **33,** 1482–1498.

Brown, R.J.S., 1980. Connection between formation factor for electrical resistivity and fluid-solid coupling factor in Biot's equations for acoustic waves in fluid-filled porous media, *Geophysics,* **45,** 1269–1275.

Cheng, C.H., Toksöz, M.N. & Willis, M.E., 1982. Determination of in situ attenuation from full waveform acoustic logs, *J. geophys. Res.,* **87,** 5477–5484.

Glover, P.W.J., Walker, E. & Jackson, M.D., 2012. Streaming-potential coefficient of reservoir rock: A theoretical model, *Geophysics,* **77,** D17–D43.

Gomez, C.T., Dvorkin, J. & Vanorio, T., 2010. Laboratory measurements of porosity, permeability, resistivity, and velocity on Fontainebleau sandstones, *Geophysics,* **75,** E191–E204.

Guan, W. & Hu, H.S., 2008. Finite-difference modeling of the electroseismic logging in a fluid-Saturated porous formation, *J. Comput. Phys.,* **227,** 5633–5648.

Guan, W., Hu, H.S. & Wang, Z., 2013a. Permeability inversion from low-frequency seismoelectric logs in fluid-saturated porous formations, *Geophys. Prospect.,* **61,** 120–133.

Guan, W., Hu, H.S. & Zheng, X.B., 2013b. Theoretical simulation of the multipole seismoelectric logging while drilling, *Geophys. J. Int.,* **195,** 1239–1250.

Haartsen, M.W. & Pride, S.R., 1997. Electroseismic waves from point sources in layered media, *J. geophys. Res.,* **102,** 24 745—24 769.

Hu, H.S. & Liu, J., 2002. Simulation of the converted electric field during acoustoelectric logging, in *72nd SEG Annual International Meeting,* Salt Lake City, Utah, USA, *Expanded Abstracts*, **21,** 348–351.

Hu, H.S., Wang, K.X. & Wang, J.N., 2000. Simulation of acoustically induced electromagnetic field in a borehole embedded in a porous formation, Borehole Acoustics Annual Report, Earth Resources Laboratory, Massachusetts Institute of Technology, **13**.1–13.30.

Hu, H.S., Guan, W. & Harris, J.M., 2007. Theoretical simulation of electroacoustic borehole logging in a fluid-Saturated porous formation, *J. acoust. Soc. Am.,* **122,** 135–145.

Hunt, C.W. & Worthington, M.H., 2000. Borehole electrokinetic responses in fracture dominated hydraulically conductive zones, *Geophys. Res. Lett.,* **27,** 1315–1318.

Johnson, D.L., Plona, T.J., Scala, C., Pasierb, F. & Kojima, H., 1982. Tortuosity and acoustic slow waves, *Phys. Rev. Lett.,* **49,** 1840–1844.

Johnson, D.L., Koplik, J. & Dashen, R., 1987. Theory of dynamic permeability and tortuosity in fluid-saturated porous media, *J. Fluid Mech.,* **176,** 379–402.

Kozeny, J., 1927. Uber kapillare Leitung der Wasser in Boden, *Sitzungsber. Akad. Wiss. Wien,* **136,** 271–306.

Leroy, P. & Revil, A., 2004. A triple-layer model of the surface electrochemical properties of clay minerals, *J. Colloid Interface Sci.,* **270,** 371–380.

Mavko, G., Mukerji, T. & Dvorikin, J., 1998. *The Rock Physics Handbook: Tools for Seismic Analysis in Porous Media,* Cambridge Univ. Press.

Mikhailov, O.V., Queen, J. & Toksöz, M.N., 2000. Using borehole electroseismic measurements to detect and characterize fractured (permeable) zones, *Geophysics,* **65,** 1098–1112.

Olsen, C., Hongdul, T. & Fabricius, I.L., 2008. Prediction of Archie's cementation factor from porosity and permeability through specific surface, *Geophysics,* **73**(2), E81–E87.

Pain, C.C., Saunders, J.H., Worthington, M.H., Singer, J.M., Stuart-Bruges, W., Mason, G. & Goddard, A., 2005. A mixed finite-element method for solving the poroelastic Biot equations with electrokinetic coupling, *Geophys. J. Int.,* **160,** 592–608.

Plyshchenkov, B.D. & Nikitin, A.A., 2010. Borehole acoustic and electric Stoneley waves and permeability, *J. Comput. Acoust.,* **18,** 87–115.

Pride, S.R., 1994. Governing equations for the coupled electromagnetics and acoustics of porous media, *Physi. Rev. B,* **50,** 15 678–15 696.

Pride, S.R. & Morgan, F., 1991. Electrokinetic dissipation induced by seismic waves, *Geophysics,* **56,** 914–925.

Revil, A., 2013. On charge accumulation in heterogeneous porous rocks under the influence of an external electric field, *Geophysics,* **78,** D217–D219.

Revil, A. & Cathles, L.M., 1999. Permeability of shaly sands, *Water Resour. Res.,* **35,** 651–662.

Revil, A. & Glover, P.W.J., 1997. Theory of ionic-surface electrical conduction in porous media, *Phys. Rev. B,* **55,** 1757–1773.

Revil, A., Pezard, P.A. & Glover, P.W.J., 1999. Streaming potential in porous media 1. Theory of the zeta potential, *J. geophys. Res.,* **104**(B9), 20 021–20 031.

Revil, A., Woodruff, W.F. & Lu, N., 2011. Constitutive equations for coupled flows in clay materials, *Water Resour. Res.,* **47,** W05548, doi:10.1029/2010WR010002.

Revil, A., Kessouri, P. & Torres-Verdín, C., 2014. Electrical conductivity, induced polarization, and permeability of the Fontainebleau sandstone. *Geophysics,* **79,** D301–D318.

Singer, J., Saunders, J., Holloway, L., Stoll, J.B., Pain, C.C., Stuart-Bruges, W. & Mason, G., 2005. Electrokinetic logging has the potential to measure permeability, in *46th SPWA Annual Logging Symposium,* New Orleans, LA, USA.

Tang, X.M., Cheng, C.H. & Toksöz, M.N., 1991. Dynamic permeability and borehole Stoneley waves: A simplified Biot-Rosenbaum model, *J. acoust. Soc. Am.,* **90,** 1632–1646.

Vernik, L., 1994. Predicting lithology and transport properties from acoustic velocities based on petrophysical classification of siliclastics, *Geophysics,* **59,** 420–427.

Wang, Z., 2010. Component wave analysis of borehole seismoelectric wavefields in a porous formation, *Master's thesis,* Harbin Institute of Technology, China.

Wu, X.Y., Wang, K.X., Guo, L., Yu, S.C. & Dong, Q.D., 1995. Inversion of permeability from the full waveform acoustic logging data, *Chin. J. Geophys. (in Chinese),* **38**(Suppl.I), 224–231.

Zhu, Z.Y. & Toksöz, M.N., 2003. Crosshole seismoelectric measurements in borehole models with fractures, *Geophysics,* **68,** 1519–1524.

Zhu, Z.Y. & Toksöz, M.N., 2005. Seismoelectric and seismomagnetic measurements in fractured borehole models, *Geophysics,* **70,** F45–F51.

Zhu, Z.Y. & Toksöz, M.N., 2015. Seismoelectric measurements in a porous quarts-sand sample with anisotropic permeability, *Geophys. Prospect.,* doi:10.1111/1365-2478.12304.

Zhu, Z.Y., Haartsen, M.W. & Toksöz, M.N., 1999. Experimental studies of electrokinetic conversions in fluid-saturated borehole models, *Geophysics,* **64,** 1349–1356.